

---

# Premier-TACO is a Few-Shot Policy Learner: Pretraining Multitask Representation via Temporal Action-Driven Contrastive Loss

---

Anonymous Author(s)

Affiliation

Address

email

## Abstract

1 We introduce Premier-TACO, a novel multitask feature representation learning  
2 methodology aiming to enhance the efficiency of few-shot policy learning in  
3 sequential decision-making tasks. Premier-TACO pretrains a general feature rep-  
4 resentation using a small subset of relevant multitask offline datasets, capturing  
5 essential environmental dynamics. This representation can then be fine-tuned to  
6 specific tasks with few expert demonstrations. Building upon the recent temporal  
7 action contrastive learning (TACO) objective, which obtains the state of art per-  
8 formance in visual control tasks, Premier-TACO additionally employs a simple  
9 yet effective negative example sampling strategy. This key modification ensures  
10 computational efficiency and scalability for large-scale multitask offline pretrain-  
11 ing. Experimental results from both Deepmind Control Suite and MetaWorld  
12 domains underscore the effectiveness of Premier-TACO for pretraining visual  
13 representation, facilitating efficient few-shot imitation learning of unseen tasks.

## 14 1 Introduction

15 Just as foundation models in language, like BERT [5] and GPT [22, 3], have revolutionized natural  
16 language processing by leveraging vast amounts of textual data to understand linguistic nuances,  
17 *pretrained foundation models* hold similar promise for sequential decision-making (SDM). In SDM,  
18 where decisions are influenced by a complex interplay of past actions, current states, and future  
19 possibilities, a pretrained foundation model can provide a rich, generalized understanding of decision  
20 sequences. This foundational knowledge, built upon diverse decision-making scenarios, can then be  
21 fine-tuned to specific tasks, much like how language models are adapted to specific linguistic tasks.

22 The following **challenges** are unique to sequential decision-making, setting it apart from existing  
23 vision and language pretraining paradigms. **(C1) Data Distribution Shift:** Training data usually  
24 consists of specific behavior-policy-generated trajectories. This leads to vastly different data dis-  
25 tributions at various stages—pretraining, finetuning, and deployment—resulting in compromised  
26 performance [14]. **(C2) Task Heterogeneity:** Unlike language and vision tasks, which often share  
27 semantic features, decision-making tasks vary widely in configurations, transition dynamics, and  
28 state and action spaces. This makes it difficult to develop a universally applicable representation.  
29 **(C3) Data Quality and Supervision:** Effective representation learning often relies on high-quality  
30 data and expert guidance. However, these resources are either absent or too costly to obtain in  
31 many real-world decision-making tasks [2, 27]. Our **aspirational criteria** for foundation model  
32 for sequential decision-making encompass several key features: **(W1) Versatility** that allows the

33 model to generalize across a wide array of tasks, even those not previously encountered, such as  
 34 new embodiments viewed or observations from novel camera angles; **(W2) Efficiency** in adapting to  
 35 downstream tasks, requiring minimal data through few-shot learning techniques; **(W3) Robustness**  
 36 to pretraining data of fluctuating quality, ensuring a resilient foundation; and **(W4) Compatibility**  
 37 with existing large pretrained models such as [20].

38 In this paper, rather than focusing on leveraging large computational vision datasets [20, 16, 15]  
 39 that overlook control-relevant considerations and suffer from a domain gap between pre-training  
 40 datasets and downstream visuo-motor tasks, we propose a novel control-centric objective function  
 41 for pretraining. Our approach, called Premier-TACO (pretraining multitask representation via  
 42 temporal action-driven contrastive loss), employs a temporal action-driven contrastive loss function  
 43 for pretraining. Unlike TACO, which treats every data point in the batch as a potential negative  
 44 example, Premier-TACO samples one negative example from a nearby window of the next state,  
 45 yielding a negative example that is visually similar to the positive one. Consequently, the latent  
 46 representation must encapsulate control-relevant information to differentiate between the positive  
 47 and negative examples, rather than depending on irrelevant features such as visual appearance.  
 48 This simple yet effective negative example sampling strategy incurs zero computational overhead,  
 49 allowing for effortless scalability in multitask offline pretraining. Through extensive empirical  
 50 evaluation, we demonstrate the **versatility** and **efficiency** of Premier-TACO’s representations in  
 51 terms of generalization to downstream tasks involving unseen embodiments and views, **robustness**  
 52 to low-quality data and **compatibility** for finetuning a pretrained visual encoder such as R3M [20],  
 53 resulting in an average performance improvement of approximately 50% across the evaluated tasks.

## 54 2 Preliminary

55 **TACO: Temporal Action Driven Contrastive Learning Objective** Temporal Action-driven Con-  
 56 trastive Learning (TACO) [40] is a reinforcement learning algorithm proposed for addressing the  
 57 representation learning problem in visual continuous control. It aims to maximize the mutual infor-  
 58 mation between representations of current states paired with action sequences and representations of  
 59 the corresponding future states:

$$\mathbb{J}_{\text{TACO}} = \mathcal{I}(Z_{t+K}; [Z_t, U_t, \dots, U_{t+K-1}]) \quad (1)$$

60 Here,  $Z_t = \phi(X_t)$  and  $U_t = \psi(A_t)$  represents latent state and action variables. Theoretically, it could  
 61 be shown that maximization of this mutual information objective leads to state and action represen-  
 62 tations that are capable of representing the optimal value functions. Empirically, TACO estimates the  
 63 lower bound of the mutual information objective by the InfoNCE loss, and it achieves the state of the  
 64 art performance for both online and offline visual continuous control, demonstrating the effectiveness  
 65 of temporal contrastive learning for representation learning in sequential decision making problems.

## 66 3 Method

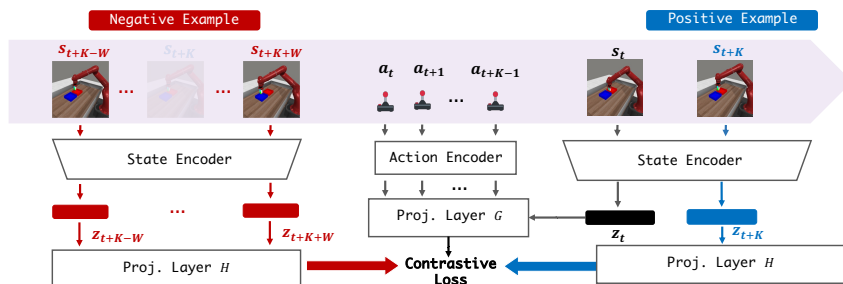


**Figure 1:** An illustration of Premier-TACO contrastive loss design. The two ‘State Encoder’s are identical, as are the two ‘Proj. Layer H’s. One negative example is sampled from the neighbors of framework  $s_{t+K}$ .

67 We introduce Premier-TACO, a generalized pre-training approach specifically formulated to tackle  
 68 the multi-task pre-training problem, enhancing sample efficiency and generalization ability for

69 downstream tasks. Building upon the success of temporal contrastive loss, exemplified by TACO [40],  
 70 in acquiring latent state representations that encapsulate individual task dynamics, our aim is to foster  
 71 representation learning that effectively captures the intrinsic dynamics spanning a diverse set of tasks  
 72 found in offline datasets. Our overarching objective is to ensure that these learned representations  
 73 exhibit the versatility to generalize across unseen tasks that share the underlying dynamic structures.

74 Nevertheless, when adapted for multitask offline pre-training, the online learning objective of  
 75 TACO [40] poses a notable challenge. Specifically, TACO’s mechanism, which utilizes the  
 76 InfoNCE [32] loss, categorizes all subsequent states  $s_{t+k}$  in the batch as negative examples. While  
 77 this methodology has proven effective in single-task reinforcement learning scenarios, it encounters  
 78 difficulties when extended to a multitask context. During multitask offline pretraining, image  
 79 observations within a batch can come from different tasks with vastly different visual appearances,  
 80 rendering the contrastive InfoNCE loss significantly less effective.

81 **Offline Pretraining Objective.** We propose a straight-  
 82 forward yet highly effective mechanism for selecting  
 83 challenging negative examples. Instead of treating  
 84 all the remaining examples in the batch as negatives,  
 85 Premier-TACO selects the negative example from a win-  
 86 dows centered at state  $s_{t+k}$  within the same episode.

87 This approach is both computationally efficient and more  
 88 statistically powerful due to negative examples which are  
 89 challenging to distinguish from similar positive examples  
 90 forcing the model to capture temporal dynamics differen-  
 91 tiating between positive and negative examples. Specifi-  
 92 cally, given a batch of state and action sequence transitions  $\{(s_t^{(i)}, [a_t^{(i)}, \dots, a_{t+K-1}^{(i)}], s_{t+K}^{(i)})\}_{i=1}^N$ , let  
 93  $z_t^{(i)} = \phi(s_t^{(i)})$ ,  $u_t^{(i)} = \psi(a_t^{(i)})$  be latent state and latent action embeddings respectively. Furthermore,  
 94 let  $\widetilde{s_{t+K}^{(i)}}$  be a negative example uniformly sampled from the window of size  $W$  centered at  $s_{t+K}$ :  
 95  $(s_{t+K-W}, \dots, s_{t+K-1}, s_{t+K+1}, \dots, s_{t+K+W})$  with  $\widetilde{z_t^{(i)}} = \phi(\widetilde{s_{t+K}^{(i)}})$  a negative latent state. Given these,  
 96 define  $g_t^{(i)} = G_\theta(z_t^{(i)}, u_t^{(i)}, \dots, u_{t+K-1}^{(i)})$ ,  $h_t^{(i)} = H_\theta(z_{t+K}^{(i)})$ , and  $\widetilde{h_t^{(i)}} = H_\theta(\widetilde{z_{t+K}^{(i)}})$  as embeddings  
 97 of future predicted and actual latent states. We optimize:

$$\mathcal{J}_{\text{Premier-TACO}}(\phi, \psi, G_\theta, H_\theta) = -\frac{1}{N} \sum_{i=1}^N \log \frac{g_t^{(i)\top} h_{t+K}^{(i)}}{g_t^{(i)\top} h_{t+K}^{(i)} + \widetilde{g_t^{(i)}}^\top \widetilde{h_{t+K}^{(i)}}}. \quad (2)$$

98

## 99 4 Experiment

100 In our empirical evaluations, we consider two benchmarks, Deepmind Control Suite [31] for locomotion  
 101 control as well as MetaWorld [37] for robotic manipulation tasks. The visualization of pretrain  
 102 and test tasks on different domains is shown in Figure 4.

103 **Setup and Baselines.** The detailed introduction of pretrained tasks for Premier-TACO and baselines  
 104 in our comparison can be found in Appendix C.1.

105 **Pretrained feature representation by Premier-TACO facilitates effective few-shot adaptation  
 106 to unseen tasks.** We measure the performance of pretrained visual representations for few-shot im-  
 107 itation learning of unseen downstream tasks in both DMC and MetaWorld. Note that we only  
 108 use  $\frac{1}{5}$  of the number of expert trajectories used in [16] and  $\frac{1}{10}$  of those used in [29]. In Ta-  
 109 ble 1, we present the results for Deepmind Control Suite. The results for MetaWorld are provided  
 110 in Table 2 of Appendix C. As shown here, pretrained representation of Premier-TACO signifi-  
 111 cantly improves the few-shot imitation learning performance compared with Learn-from-scratch,  
 112 with a **101%** improvement on Deepmind Control Suite and **74%** improvement on MetaWorld,  
 113 respectively. Moreover, it also outperforms all the baselines across all tasks by a large margin.

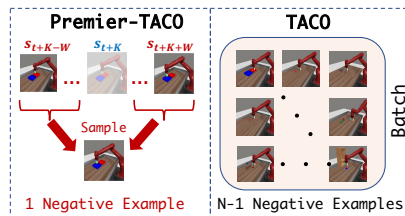


Figure 2: Difference between Premier-TACO and TACO for sampling negative examples

DMControl		Models								
Tasks		LFS	SMART	Best PVRs	TD3+BC	Inverse	CURL	ATC	SPR	Premier-TACO
Seen Embodiments	Finger Spin	34.8±3.4	44.2±8.2	38.4±9.3	68.8±7.1	33.4±8.4	35.1±9.6	51.1±9.4	55.9±6.2	<b>75.2 ± 0.6</b>
	Hopper Hop	8.0 ± 1.3	14.2 ± 3.9	23.2 ± 4.9	49.1 ± 4.3	48.3 ± 5.2	28.7 ± 5.2	34.9 ± 3.9	52.3 ± 7.8	<b>75.3 ± 4.6</b>
	Walker Walk	30.4±2.9	54.1±5.2	32.6±8.7	65.8±2.0	64.4±5.6	37.3±7.9	44.6±5.0	72.9±1.5	<b>88.0 ± 0.8</b>
	Humanoid Walk	15.1±1.3	18.4±3.9	30.1±7.5	34.9±8.5	41.9±8.4	19.4±2.8	35.1±3.1	30.1±6.2	<b>51.4 ± 4.9</b>
Unseen Embodiments	Dog Trot	52.7±3.5	59.7±5.2	73.5±6.4	82.3±4.4	85.3±2.1	71.9±2.2	84.3±0.5	79.9±3.8	<b>93.9 ± 5.4</b>
	Cup Catch	56.8±5.6	66.8±6.2	93.7±1.8	97.1±1.7	96.7±2.6	96.7±2.6	96.2±1.4	96.9±3.1	<b>98.9 ± 0.1</b>
	Reacher Hard	34.6±4.1	52.1±3.8	64.9±5.8	59.6±9.9	61.7±4.6	50.4±4.6	56.9±9.8	62.5±7.8	<b>81.3 ± 1.8</b>
	Cheetah Run	25.1±2.9	41.1±7.2	39.5±9.7	50.9±2.6	51.5±5.5	36.8±5.4	30.1±1.0	40.2±9.6	<b>65.7 ± 1.1</b>
Unseen Embodiments	Quadruped Walk	61.1±5.7	45.4±4.3	63.2±4.0	76.6±7.4	82.4±6.7	72.8±8.9	81.9±5.6	65.6±4.0	<b>83.2 ± 5.7</b>
	Quadruped Run	45.0±2.9	27.9±5.3	64.0±2.4	48.2±5.2	52.1±1.8	55.1±5.4	2.6±3.6	68.2±3.2	<b>76.8 ± 7.5</b>
Mean Performance		38.2	42.9	52.3	63.3	61.7	50.4	52.7	62.4	<b>79.0</b>

**Table 1: [(W1) Versatility (W2) Efficiency] Few-shot Behavior Cloning (BC) for unseen task of DMC.** Performance (Agent Reward / Expert Reward) of baselines and Premier-TACO on 10 unseen tasks on Deepmind Control Suite. **Bold** numbers indicate the best results. Agent Policies are evaluated every 1000 gradient steps for a total of 100000 gradient steps and we report the average performance over the 3 best epochs over the course of learning. Premier-TACO outperforms all the baselines, showcasing its superior efficacy in generalizing to unseen tasks with seen or **unseen embodiments**.

114 Premier-TACO **pre-trained representation enables knowledge**  
 115 **sharing across different embodiments.** Ideally, a resilient and  
 116 generalizable state feature representation ought not only to encapsu-  
 117 late universally applicable features for a given embodiment across a  
 118 variety of tasks, but also to exhibit the capability to generalize across  
 119 distinct embodiments. Here, we evaluate the few-shot behavior  
 120 cloning performance of Premier-TACO pre-trained encoder from  
 121 **DMC-6** on four tasks featuring unseen embodiments: Cup Catch,  
 122 Cheetah Run, and Quadruped Walk. In comparison to Learn-  
 123 from-scratch, as shown in Table 1, Premier-TACO pre-trained  
 124 representation realizes an **82%** performance gain, demonstrating  
 125 the robust generalizability of our pre-trained feature representations.

126 Premier-TACO **Pretrained Representation is also generalizable**  
 127 **to unseen tasks with camera views.** Beyond generalizing to unseen  
 128 embodiments, an ideal robust visual representation should possess  
 129 the capacity to adapt to unfamiliar tasks under novel camera views. In Figure 3, we evaluate the  
 130 five-shot learning performance of our model on four previously unseen tasks in MetaWorld with a  
 131 new view. In particular, during pretraining, the data from MetaWorld are generated using the same  
 132 view as employed in [10, 26]. Then for downstream policy learning, the agent is given five expert  
 133 trajectories under a different corner camera view, as depicted in the figure. Notably, Premier-TACO  
 134 also achieves a substantial performance enhancement, thereby underscoring the robust generalizability  
 135 of our pretrained visual representation.

136 **Robustness to low-quality pretraining data.** To further study the resilience of Premier-TACO, we  
 137 employ low-quality data to train Premier-TACO representations in Appendix C.3.

138 **Compatibility: Pretrained visual encoder finetuning with Premier-TACO.** To further validate the  
 139 compatibility of our Premier-TACO approach, we compared the results of R3M with no fine-tuning,  
 140 in-domain fine-tuning [9], and fine-tuning using our method on selected Deepmind Control Suite and  
 141 MetaWorld pretraining tasks. Results in Appendix C.4 unequivocally demonstrate that direct fine-  
 142 tuning on in-domain tasks leads to a performance decline across multiple tasks. However, leveraging  
 143 the Premier-TACO learning objective for fine-tuning substantially enhances the performance of  
 144 R3M. This not only underscores the role of our method in bridging the domain gap and capturing  
 145 essential control features but also highlights its robust generalization capabilities. Furthermore, these  
 146 findings strongly suggest that our Premier-TACO approach is highly adaptable to a wide range of  
 147 multi-task pretraining scenarios, irrespective of the model’s size or the size of the pretrained data.

148 **Ablation Studies.** Ablation experiments for batch sizes and window sizes are in Appendix D.

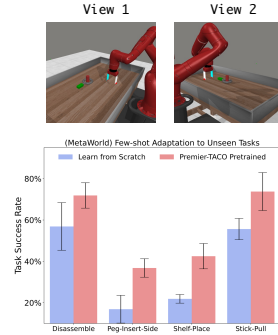


**Figure 3: [(W1) Versatility] MetaWorld: Few-shot adaptation to unseen tasks from an unseen camera view.**

## 149 A Problem Setting

### 150 A.1 Multitask Offline Pretraining

151 We consider a collection of tasks  $\{\mathcal{T}_i : (\mathcal{X}, \mathcal{A}_i, \mathcal{P}_i, \mathcal{R}_i, \gamma)\}_{i=1}^N$  with the same dimensionality in ob-  
152 servation space  $\mathcal{X}$ . Let  $\phi : \mathcal{X} \rightarrow \mathcal{Z}$  be a representation function of the agent’s observation, which is  
153 either randomly initialized or pre-trained already on a large-scale vision dataset such as ImageNet [4]  
154 or Ego4D [7]. Assuming that the agent is given a multitask offline dataset  $\{(x_i, a_i, x'_i, r_i)\}$  of a  
155 subset of  $K$  tasks  $\{\mathcal{T}_{n_j}\}_{j=1}^K$ . The objective is to pretrain a generalizable state representation  $\phi$  or  
156 a motor policy  $\pi$  so that when facing an unseen downstream task, it could quickly adapt with few  
157 expert demonstrations, using the pretrained representation.

158 Below we summarize the pretraining and finetuning setups.

159 **Pretraining:** The agent get access to a multitask offline dataset, which could be highly suboptimal.  
160 The goal is to learn a generalizable shared state representation from pixel inputs.

161 **Adaptation:** Adapt to unseen downstream task from few expert demonstration with imitation learning.

## 162 B Related Work

163 **Pretraining Visual Representations.** Existing works apply self-supervised pre-training from rich  
164 vision data to build foundation models. However, applying this approach to sequential decision-  
165 making tasks is challenging. Recent works have explored large-scale pre-training with offline data in  
166 the context of reinforcement learning. Efforts such as R3M [20], VIP [15], MVP [34], PIE-G [38],  
167 and VC-1 [16] highlight this direction. However, there’s a notable gap between the datasets used for  
168 pre-training and the actual downstream tasks. In fact, a recent study [9] found that models trained  
169 from scratch can often perform better than those using pre-trained representations, suggesting the  
170 limitation of these approaches. It’s important to acknowledge that these pre-trained representations  
171 are not control-relevant, and they lack explicit learning of a latent world model. In contrast to these  
172 prior approaches, our pretrained representations learn to capture the control-relevant features with an  
173 effective temporal contrastive learning objective.

174 For control tasks, several pretraining frameworks have emerged to model state-action interactions from  
175 high-dimensional observations by leveraging causal attention mechanisms. SMART [29] introduces a  
176 self-supervised and control-centric objective to train transformer-based models for multitask decision-  
177 making, although it requires additional fine-tuning with large number of demonstrations during  
178 downstream time. As an improvement, DualMind [33] pretrains representations using 45 tasks for  
179 general-purpose decision-making without task-specific fine-tuning. Besides, some methods [25, 18,  
180 35, 30] first learn a general representation by exploring the environment online, and then use this  
181 representation to train the policy on downstream tasks. In comparison, our approach is notably  
182 more efficient and doesn’t require training with such an extensive task set. Nevertheless, we provide  
183 empirical evidence demonstrating that our method can effectively handle multi-task pretraining.

184 **Contrastive Representation for Visual RL** Contrastive learning is a self-supervised technique that  
185 leverages similarity constraints between data to learn effective representations (embeddings), and it  
186 has demonstrated remarkable success across various domains. In the context of visual reinforcement  
187 learning (RL), contrastive learning plays a pivotal role in training robust state representations from  
188 raw visual inputs, thereby enhancing sample efficiency. CURL [13] extracts high-level features by  
189 utilizing InfoNCE[32] to maximize agreement between augmented observations, although it does  
190 not explicitly consider temporal relationships between states. Several approaches, such as CPC [11],  
191 ST-DIM [1], and ATC [28], introduce temporal dynamics into the contrastive loss. They do so  
192 by maximizing mutual information between states with short temporal intervals, facilitating the  
193 capture of temporal dependencies. DRIML [17] proposes a policy-dependent auxiliary objective  
194 that enhances agreement between representations of consecutive states, specifically considering the  
195 first action of the action sequence. Recent advancements by [12, 39] incorporate actions into the  
196 contrastive loss, emphasizing behavioral similarity. TACO [40] takes a step further by learning both  
197 state and action representations. It optimizes the mutual information between the representations of

198 current states paired with action sequences and the representations of corresponding future states.  
 199 In our approach, we build upon the efficient extension of TACO, harnessing the full potential of  
 200 state and action representations for downstream tasks. On the theory side, the Homer algorithm [19]  
 201 uses a binary temporal contrastive objective reminiscent of the approach used here, which differs  
 202 by abstracting actions as well states, using an ancillary embedding, removing leveling from the  
 203 construction, and of course extensive empirical validation.

## 204 C Experiments

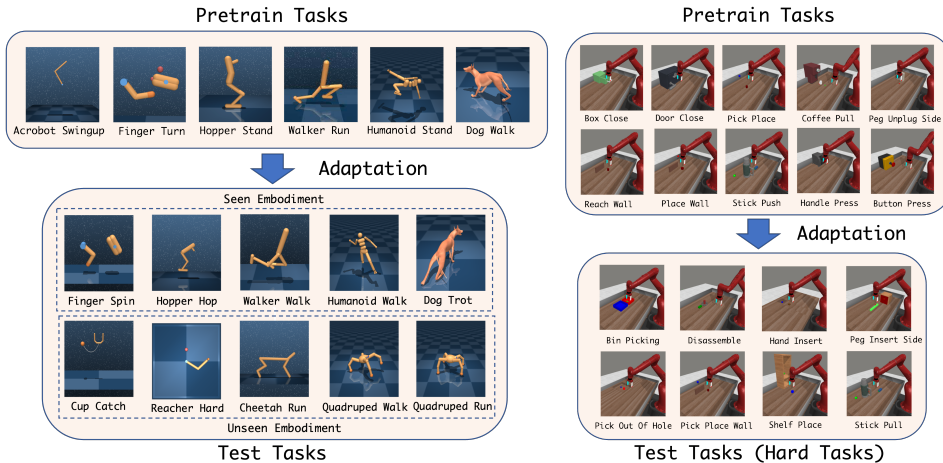


**Figure 4:** Pretrain and Test Tasks split for Deepmind Control Suite and MetaWorld. The left figures are Deepmind Control Suite tasks and the right figures MetaWorld tasks.

### 205 C.1 Experiment Setup

206 **Deepmind Control Suite (DMC) [31]:** We consider a selection of 16 challenging tasks from  
 207 Deepmind Control Suite. Note that compared with prior works such as [16, 29], we consider much  
 208 harder tasks, including ones from the humanoid and dog domains, which feature intricate kinematics,  
 209 skinning weights and collision geometry. For pretraining, we select six tasks (**DMC-6**), including  
 210 Acrobot Swingup, Finger Turn Hard, Hopper Stand, Walker Run, Humanoid Walk, and Dog Stand.  
 211 We generate an exploratory dataset for each task by sampling trajectories generated in exploratory  
 212 stages of a DrQ-v2 [36] learning agent. In particular, we sample 1000 trajectories from the online  
 213 replay buffer of DrQ-v2 once it reaches the convergence performance. This ensures the diversity of  
 214 the pretraining data, but in practice, such a high-quality dataset could be hard to obtain. So, later  
 215 in the experiments, we will also relax this assumption and consider pretrained trajectories that are  
 216 sampled from uniformly random actions.

217 **MetaWorld [37]:** We select a set of 10 tasks for pretraining, which encompasses a variety of motion  
 218 patterns of the Sawyer robotic arm and interaction with different objects. To collect an exploratory  
 219 dataset for pretraining, we execute the scripted policy with Gaussian noise of a standard deviation of  
 220 0.3 added to the action. By adding such a noise, the success rate of collected policies on average is  
 221 only around 20% across ten pretrained human tasks.

222 **Baselines.** We compare Premier-TACO with the following representation pretraining baselines:

- 223  $\triangleright$  Learn from Scratch: Behavior Cloning with randomly initialized shallow ConvNet encoder.  
 224 Different from [20, 16], which use a randomly initialized ResNet for evaluation, we find that  
 225 using a shallow network with an input image size of  $84 \times 84$  on both Deepmind Control Suite  
 226 and MetaWorld yields superior performance. Additionally, we also include data augmentation  
 227 into behavior cloning following [9].
- 228  $\triangleright$  Policy Pretraining: We first train a multitask policy by TD3+BC [6] on the pretraining dataset.  
 229 While numerous alternative offline RL algorithms exist, we choose TD3+BC as a representative

MetaWorld		Models							
Unseen Tasks	LfS	SMART	Best PVRs	TD3+BC	Inverse	CURL	ATC	SPR	Premier-TACO
Bin Picking	62.5 ± 12.5	71.3 ± 9.6	60.2 ± 4.3	50.6 ± 3.7	55.0 ± 7.9	45.6 ± 5.6	55.6 ± 7.8	67.9 ± 6.4	<b>78.5 ± 7.2</b>
Disassemble	56.3 ± 6.5	52.9 ± 4.5	70.4 ± 8.9	56.9 ± 11.5	53.8 ± 8.1	66.2 ± 8.3	45.6 ± 9.8	48.8 ± 5.4	<b>86.7 ± 8.9</b>
Hand Insert	34.7 ± 7.5	34.1 ± 5.2	35.5 ± 2.3	46.2 ± 5.2	50.0 ± 3.5	49.4 ± 7.6	51.2 ± 1.3	52.4 ± 5.2	<b>75.0 ± 7.1</b>
Peg Insert Side	28.7 ± 2.0	20.9 ± 3.6	48.2 ± 3.6	30.0 ± 6.1	33.1 ± 6.2	28.1 ± 3.7	31.8 ± 4.8	39.2 ± 7.4	<b>62.7 ± 4.7</b>
Pick Out Of Hole	53.7 ± 6.7	65.9 ± 7.8	66.3 ± 7.2	46.9 ± 7.4	50.6 ± 5.1	43.1 ± 6.2	54.4 ± 8.5	55.3 ± 6.8	<b>72.7 ± 7.25</b>
Pick Place Wall	40.5 ± 4.5	62.8 ± 5.9	63.2 ± 9.8	63.8 ± 12.4	71.3 ± 11.3	73.8 ± 11.9	68.7 ± 5.5	72.3 ± 7.5	<b>80.2 ± 8.2</b>
Shelf Place	26.3 ± 4.1	57.9 ± 4.5	32.4 ± 6.5	45.0 ± 7.7	36.9 ± 6.7	35.0 ± 10.8	35.6 ± 10.7	38.0 ± 6.5	<b>70.4 ± 8.1</b>
Stick Pull	46.3 ± 7.2	65.8 ± 8.2	52.4 ± 5.6	72.3 ± 11.9	57.5 ± 9.5	43.1 ± 15.2	72.5 ± 8.9	68.5 ± 9.4	<b>80.0 ± 8.1</b>
<b>Mean</b>	43.6	53.9	53.6	51.5	51.0	48.3	51.9	55.3	<b>75.8</b>

**Table 2: [(W1) Versatility (W2) Efficiency] Five-shot Behavior Cloning (BC) for unseen task of MetaWorld.** Success rate of Premier-TACO and baselines across 8 hard unseen tasks on MetaWorld. Results are aggregated over 4 random seeds. **Bold** numbers indicate the best results.

230 due to its simplicity and great empirical performance. After pretraining, we take the pretrained  
 231 ConvNet encoder and drop the policy MLP layers.

232 ▷ Pretrained Visual Representations (PVRs): We evaluate the state-of-the-art frozen pretrained  
 233 visual representations including PVR [21], MVP [34], R3M [20] and VC-1 [16], and report the  
 234 best performance of these PVRs models for each task.

235 ▷ Control Transformer: SMART [29] is a self-supervised representation pretraining framework  
 236 which utilizes a masked prediction objective for pretraining representation under Decision  
 237 Transformer architecture, and then use the pretrained representation to learn policies for  
 238 downstream tasks.

239 ▷ Inverse Dynamics Model: We pretrain an inverse dynamics model to predict actions and use  
 240 the pretrained representation for downstream task.

241 ▷ Contrastive/Self-supervised Learning Objectives: CURL [13], ATC [28], and SPR [23, 24].  
 242 CURL and ATC are two approaches that apply contrastive learning into sequential decision  
 243 making problems. While CURL treats augmented states as positive pairs, it neglects the temporal  
 244 dependency of MDP. In comparison, ATC takes the temporal structure into consideration. The  
 245 positive example of ATC is an augmented view of a temporally nearby state. SPR applies BYOL  
 246 objective [8] into sequential decision making problems by pretraining state representations that  
 247 are self-predictive of future states.

248 **Number of Demonstrations and Evaluation Metric.** For DMC, we use **20 expert trajectories**  
 249 for imitation learning except for the two hardest tasks, Humanoid Walk and Dog Trot, for which  
 250 we use 100 trajectories instead. We record the performance of the agent by calculating the ratio  
 251 of  $\frac{\text{Agent Reward}}{\text{Expert Reward}}$ , where Expert Reward is the episode reward of the expert policy used to collect  
 252 demonstration trajectories. For MetaWorld, we use **5 expert trajectories** for all eight downstream  
 253 tasks, and we use task success rate as the performance metric.

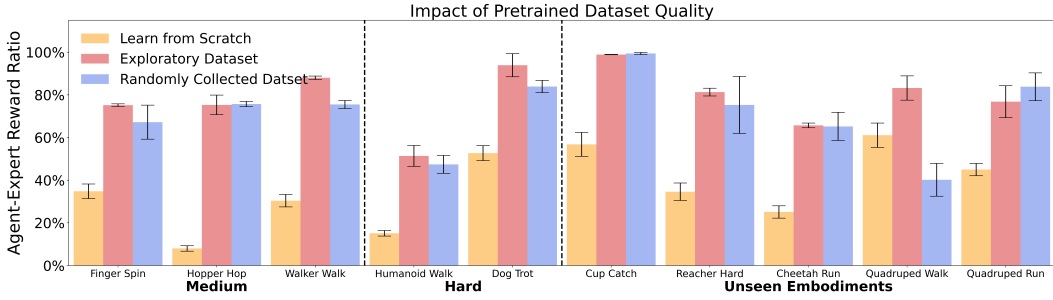
## 254 C.2 Adaptation to Unseen Tasks

255 The results of adaptation to unseen tasks in MetaWorld are shown in Table 2.

## 256 C.3 Robustness to Low-quality Data

257 Premier-TACO **Pre-trained Representation is resilient to low-quality data.** We evaluate the  
 258 resilience of Premier-TACO by employing randomly collected trajectory data from Deepmind  
 259 Control Suite for pretraining and compare it with Premier-TACO representations pretrained using  
 260 an exploratory dataset and the learn-from-scratch approach. As illustrated in Figure 5, across  
 261 all downstream tasks, even when using randomly pretrained data, the Premier-TACO pretrained  
 262 model still maintains a significant advantage over learning-from-scratch. When compared with  
 263 representations pretrained using exploratory data, there are only small disparities in a few individual  
 264 tasks, while they remain comparable in most other tasks. This strongly indicates the robustness

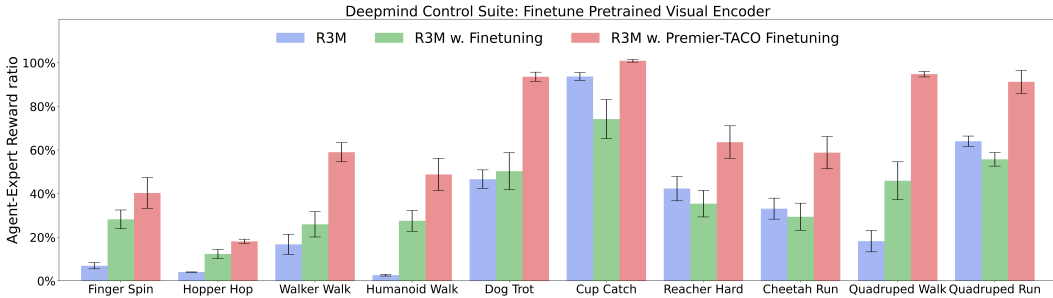
265 of Premier-TACO to low-quality data. Even without the use of expert control data, our method is  
 266 capable of extracting valuable information.



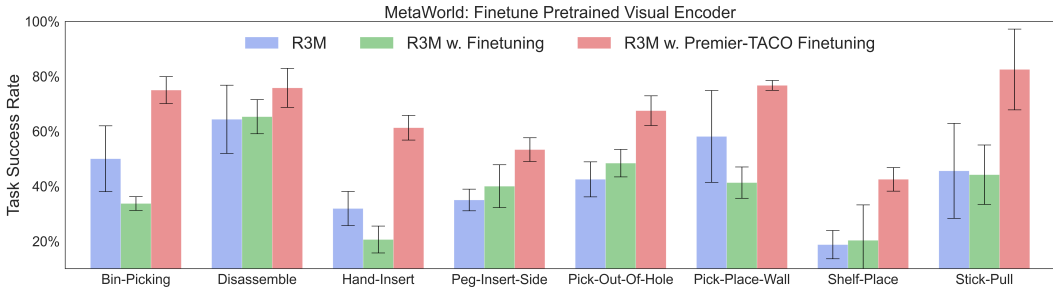
267 **Figure 5: [(W3) Robustness]** Premier-TACO pretrained with exploratory dataset vs. Premier-TACO pre-  
 268 trained with randomly collected dataset

#### 267 C.4 Finetuning on pretrained visual representations

268 We conduct fine-tuning on pretrained visual representations using in-domain control trajectories  
 269 following the Premier-TACO framework. Importantly, our findings deviate from the observations  
 270 made in prior works [9, 16], where fine-tuning of R3M [20] on in-domain demonstration data using  
 271 the task-centric behavior cloning objective, resulted in performance degradation. We speculate that  
 272 two main factors contribute to this phenomenon. First, a domain gap exists between out-of-domain  
 273 pretraining data and in-domain fine-tuning data. Second, fine-tuning with few-shot learning can lead  
 274 to overfitting for large pretrained models. Comparisons among R3M [20], R3M with in-domain  
 275 finetuning [9] and R3M finetuned with Premier-TACO in Deepmind Control Suite and MetaWorld  
 are presented in Figure 6 and 7.



276 **Figure 6: [(W4) Compatibility]** Finetune R3M [20], a generalized Pretrained Visual Encoder with  
 Premier-TACO learning objective vs. R3M with in-domain finetuning in Deepmind Control Suite and Meta-  
 World.



277 **Figure 7: [(W4) Compatibility]** Finetune R3M [20], a generalized Pretrained Visual Encoder with  
 Premier-TACO learning objective vs. R3M with in-domain finetuning in Deepmind Control Suite and Meta-  
 World.

276



## 277 D Ablation Studies

### 278 D.1 Batch Size

279 Compared with TACO, the negative example sampling strategy  
280 employed in Premier-TACO allows us to sample harder  
281 negative examples within the same episode as the positive  
282 example. We expect Premier-TACO to work much better  
283 with small batch sizes, compared with TACO where the  
284 negative examples from a given batch could be coming from  
285 various tasks and thus the batch size required would scale up  
286 linearly with the number of pretraining tasks. In our previous  
287 experimental results, Premier-TACO is pretrained with a  
288 batch size of 4096, a standard batch size used in contrastive  
289 learning literature. Here, to empirically verify the effects  
290 of different choices of the pretraining batch size, we train  
291 Premier-TACO with batch sizes other than 4096, and compare  
292 with the performance of TACO using a batch size of 4096.

293 Figure 8 displays the average performance of few-shot imitation learning across all ten tasks in  
294 the DeepMind Control Suite. As depicted in the figure, our model markedly surpasses TACO,  
295 maintaining this superiority even with a batch size of 512, and exhibits performance saturation  
296 beyond a batch size of 4096. This observation substantiates that the negative example sampling strategy  
297 employed by Premier-TACO is indeed the key for the success of multitask offline pretraining.

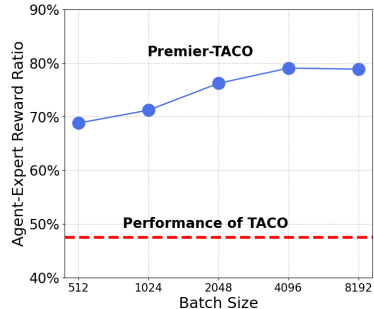


**Figure 8:** Averaged performance of Premier-TACO on 10 Deepmind Control Suite Tasks across different batch sizes.

### 298 D.2 Window Size

299 In Premier-TACO, the window size  $W$  determines the hard-  
300 ness of the negative example. A smaller window size results  
301 in negative examples that are more challenging to distinguish  
302 from positive examples, though they may become excessively  
303 difficult to differentiate in the latent space. Conversely, a larger  
304 window size makes distinguishing relatively straightforward,  
305 thereby mitigating the impacts of negative sampling. In the  
306 preceding experiments, a consistent window size of 5 was ap-  
307 plied across all trials on both the DeepMind Control Suite and  
308 MetaWorld. Here we empirically evaluate the effects of varying  
309 window sizes on the average performance of our model across  
310 ten DeepMind Control Tasks, as depicted in Figure X. Notably,  
311 our observations reveal that performance is comparable when  
312 the window size is set to 3, 5, or 7, whereas excessively small  
313 ( $W = 1$ ) or large ( $W = 9$ ) window sizes lead to worse performance.

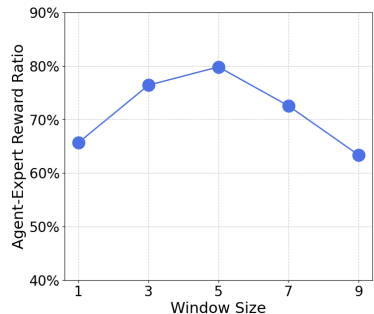


**Figure 9:** Averaged performance of Premier-TACO on 10 Deepmind Control Suite Tasks across different window sizes

## 314 E Implementation Details

315 **Dataset** For six pretraining tasks of the Deepmind Control Suite, we train visual RL agents for  
316 individual tasks with DrQ-v2 [36] until convergence, and we store all the historical interaction  
317 steps in a separate buffer. Then, we sample 200 trajectories from the buffer for all tasks except  
318 for Humanoid Stand and Dog Walk. Since these two tasks are significantly harder, we use 1000  
319 pretraining trajectories instead. Each episode in the Deepmind Control Suite consists of 500 time  
320 steps. In terms of the randomly collected dataset, we sample trajectories by taking actions with each  
321 dimension independently sampled from a uniform distribution  $\mathcal{U}(-1., 1.)$  For MetaWorld, we collect  
322 1000 trajectories for each task, where each episode consists of 200 time steps. We add a Gaussian  
323 noise of standard deviation 0.3 to the provided scripted policy.

324 **Pretraining** For the shallow convolutional network, we follow the same architecture as in (author?)  
 325 [36] and add a layer normalization on top of the output of the ConvNet encoder. We set the feature  
 326 dimension of the ConNet encoder to be 100. In total, this encoder has around 3.95 million parameters.

```

327 1 class Encoder(nn.Module):
328 2     def __init__(self):
329 3         super().__init__()
330 4         self.repr_dim = 32 * 35 * 35
331 5
332 6         self.convnet = nn.Sequential(nn.Conv2d(84, 32, 3, stride=2),
333 7                                     nn.ReLU(), nn.Conv2d(32, 32, 3, stride=1),
334 8                                     nn.ReLU(), nn.Conv2d(32, 32, 3, stride=1),
335 9                                     nn.ReLU(), nn.Conv2d(32, 32, 3, stride=1),
336 0                                     nn.ReLU())
337 1         self.trunk = nn.Sequential(nn.Linear(self.repr_dim,
338                                     feature_dim),
339 2                                     nn.LayerNorm(feature_dim), nn.Tanh())
340 3
341 4     def forward(self, obs):
342 5         obs = obs / 255.0 - 0.5
343 6         h = self.convnet(obs).view(h.shape[0], -1)
344 7         return self.trunk(h)

```

**Listing 1:** Shallow Convolutional Network Architecture Used in Premier-TACO

345 For Premier-TACO loss, the number of timesteps  $K$  is set to be 3 throughout the experiments,  
 346 and the window size  $W$  is fixed to be 5. The Action Encoder is a two-layer MLP with input size  
 347 being the action space dimensionality, hidden size being 64, and output size being the same as the  
 348 dimensionality of the action space. The projection layer  $G$  is a two-layer MLP with input size being  
 349 feature dimension plus the number of timesteps times the dimensionality of the action space. Its  
 350 hidden size is 1024. In terms of the projection layer  $H$ , it is also a two-layer MLP with input and  
 351 output size both being the feature dimension and hidden size being 1024. Throughout the experiments,  
 352 we set the batch size to be 4096 and the learning rate to be  $1e-4$ . For the contrastive/self-supervised  
 353 based baselines, CURL, ATC, and SPR, we use the same batch size of 4096 as Premier-TACO. For  
 354 Multitask TD3+BC and Inverse dynamics modeling baselines, we use a batch size of 1024.

355 **Imitation Learning** A batch size of 128 and a learning rate of  $1e-4$  are used. During behavior  
 356 cloning, we finetune the Shallow ConvNet Encoder. However, when we applied Premier-TACO for  
 357 the large pre-trained ResNet/ViT model, we keep the model weights frozen.

358 In total, we take 100,000 gradient steps and conduct evaluations for every 1000 steps. For evaluations  
 359 within the DeepMind Control Suite, we utilize the trained policy to execute 20 episodes, subse-  
 360 quently recording the mean episode reward. In the case of MetaWorld, we execute 50 episodes and  
 361 document the success rate of the trained policy. We report the average of the highest three episode  
 362 rewards/success rates from the 100 evaluated checkpoints.

363 **Computational Resources** For our experiments, we use 8 NVIDIA RTX A6000 with PyTorch  
 364 Distributed DataParallel for pretraining visual representations, and we use NVIDIA RTX2080Ti for  
 365 downstream imitation learning.

366 **References**

- 367 [1] Ankesh Anand, Evan Racah, Sherjil Ozair, Yoshua Bengio, Marc-Alexandre Côté, and R Devon  
368 Hjelm. Unsupervised state representation learning in atari. In H. Wallach, H. Larochelle,  
369 A. Beygelzimer, F. d'Alché-Buc, E. Fox, and R. Garnett, editors, *Advances in Neural Information*  
370 *Processing Systems*, volume 32. Curran Associates, Inc., 2019. 5
- 371 [2] Anthony Brohan, Noah Brown, Justice Carbajal, Yevgen Chebotar, Joseph Dabis, Chelsea  
372 Finn, Keerthana Gopalakrishnan, Karol Hausman, Alex Herzog, Jasmine Hsu, Julian Ibarz,  
373 Brian Ichter, Alex Irpan, Tomas Jackson, Sally Jesmonth, Nikhil J Joshi, Ryan Julian, Dmitry  
374 Kalashnikov, Yuheng Kuang, Isabel Leal, Kuang-Huei Lee, Sergey Levine, Yao Lu, Utsav  
375 Malla, Deeksha Manjunath, Igor Mordatch, Ofir Nachum, Carolina Parada, Jodilyn Peralta,  
376 Emily Perez, Karl Pertsch, Jornell Quiambao, Kanishka Rao, Michael Ryoo, Grecia Salazar,  
377 Pannag Sanketi, Kevin Sayed, Jaspiar Singh, Sumedh Sontakke, Austin Stone, Clayton Tan,  
378 Huong Tran, Vincent Vanhoucke, Steve Vega, Quan Vuong, Fei Xia, Ted Xiao, Peng Xu, Sichun  
379 Xu, Tianhe Yu, and Brianna Zitkovich. Rt-1: Robotics transformer for real-world control at  
380 scale, 2023. 1
- 381 [3] Tom Brown, Benjamin Mann, Nick Ryder, Melanie Subbiah, Jared D Kaplan, Prafulla Dhariwal,  
382 Arvind Neelakantan, Pranav Shyam, Girish Sastry, Amanda Askell, Sandhini Agarwal, Ariel  
383 Herbert-Voss, Gretchen Krueger, Tom Henighan, Rewon Child, Aditya Ramesh, Daniel Ziegler,  
384 Jeffrey Wu, Clemens Winter, Chris Hesse, Mark Chen, Eric Sigler, Mateusz Litwin, Scott  
385 Gray, Benjamin Chess, Jack Clark, Christopher Berner, Sam McCandlish, Alec Radford, Ilya  
386 Sutskever, and Dario Amodei. Language models are few-shot learners. In H. Larochelle,  
387 M. Ranzato, R. Hadsell, M.F. Balcan, and H. Lin, editors, *Advances in Neural Information*  
388 *Processing Systems*, volume 33, pages 1877–1901. Curran Associates, Inc., 2020. 1
- 389 [4] Jia Deng, Wei Dong, Richard Socher, Li-Jia Li, Kai Li, and Li Fei-Fei. Imagenet: A large-scale  
390 hierarchical image database. *IEEE Conference on Computer Vision and Pattern Recognition*  
391 *(CVPR)*, 2009. 5
- 392 [5] Jacob Devlin, Ming-Wei Chang, Kenton Lee, and Kristina Toutanova. BERT: Pre-training of  
393 deep bidirectional transformers for language understanding. In *Proceedings of the 2019 Confer-*  
394 *ence of the North American Chapter of the Association for Computational Linguistics: Human*  
395 *Language Technologies, Volume 1 (Long and Short Papers)*, pages 4171–4186, Minneapolis,  
396 Minnesota, June 2019. Association for Computational Linguistics. 1
- 397 [6] Scott Fujimoto and Shixiang (Shane) Gu. A minimalist approach to offline reinforcement  
398 learning. In M. Ranzato, A. Beygelzimer, Y. Dauphin, P.S. Liang, and J. Wortman Vaughan,  
399 editors, *Advances in Neural Information Processing Systems*, volume 34, pages 20132–20145.  
400 Curran Associates, Inc., 2021. 6
- 401 [7] Kristen Grauman, Andrew Westbury, Eugene Byrne, Zachary Chavis, Antonino Furnari, Ro-  
402 hit Girdhar, Jackson Hamburger, Hao Jiang, Miao Liu, Xingyu Liu, Miguel Martin, Tushar  
403 Nagarajan, Ilija Radosavovic, Santhosh Kumar Ramakrishnan, Fiona Ryan, Jayant Sharma,  
404 Michael Wray, Mengmeng Xu, Eric Zhongcong Xu, Chen Zhao, Siddhant Bansal, Dhruv  
405 Batra, Vincent Cartillier, Sean Crane, Tien Do, Morrie Doulaty, Akshay Erapalli, Christoph  
406 Feichtenhofer, Adriano Fragomeni, Qichen Fu, Abraham Gebreselasie, Cristina Gonzalez, James  
407 Hillis, Xuhua Huang, Yifei Huang, Wenqi Jia, Weslie Khoo, Jachym Kolar, Satwik Kottur,  
408 Anurag Kumar, Federico Landini, Chao Li, Yanghao Li, Zhenqiang Li, Karttikeya Mangalam,  
409 Raghava Modhugu, Jonathan Munro, Tullie Murrell, Takumi Nishiyasu, Will Price, Paola Ruiz  
410 Puentes, Mery Ramazanova, Leda Sari, Kiran Somasundaram, Audrey Southerland, Yusuke  
411 Sugano, Ruijie Tao, Minh Vo, Yuchen Wang, Xindi Wu, Takuma Yagi, Ziwei Zhao, Yunyi Zhu,  
412 Pablo Arbelaez, David Crandall, Dima Damen, Giovanni Maria Farinella, Christian Fuegen,  
413 Bernard Ghanem, Vamsi Krishna Ithapu, C. V. Jawahar, Hanbyul Joo, Kris Kitani, Haizhou  
414 Li, Richard Newcombe, Aude Oliva, Hyun Soo Park, James M. Rehg, Yoichi Sato, Jianbo

- 415 Shi, Mike Zheng Shou, Antonio Torralba, Lorenzo Torresani, Mingfei Yan, and Jitendra Malik.  
416 Ego4d: Around the world in 3,000 hours of egocentric video, 2022. [5](#)
- 417 [8] Jean-Bastien Grill, Florian Strub, Florent Alché, Corentin Tallec, Pierre Richemond, Elena  
418 Buchatskaya, Carl Doersch, Bernardo Avila Pires, Zhaohan Guo, Mohammad Gheshlaghi Azar,  
419 Bilal Piot, koray kavukcuoglu, Remi Munos, and Michal Valko. Bootstrap your own latent -  
420 a new approach to self-supervised learning. In H. Larochelle, M. Ranzato, R. Hadsell, M.F.  
421 Balcan, and H. Lin, editors, *Advances in Neural Information Processing Systems*, volume 33,  
422 pages 21271–21284. Curran Associates, Inc., 2020. [7](#)
- 423 [9] Nicklas Hansen, Zhecheng Yuan, Yanjie Ze, Tongzhou Mu, Aravind Rajeswaran, Hao Su,  
424 Huazhe Xu, and Xiaolong Wang. On pre-training for visuo-motor control: Revisiting a learning-  
425 from-scratch baseline. In *CoRL 2022 Workshop on Pre-training Robot Learning*, 2022. [4](#), [5](#), [6](#),  
426 [8](#)
- 427 [10] Nicklas A Hansen, Hao Su, and Xiaolong Wang. Temporal difference learning for model  
428 predictive control. In Kamalika Chaudhuri, Stefanie Jegelka, Le Song, Csaba Szepesvari, Gang  
429 Niu, and Sivan Sabato, editors, *Proceedings of the 39th International Conference on Machine  
430 Learning*, volume 162 of *Proceedings of Machine Learning Research*, pages 8387–8406. PMLR,  
431 17–23 Jul 2022. [4](#)
- 432 [11] Olivier Henaff. Data-efficient image recognition with contrastive predictive coding. In  
433 Hal Daumé III and Aarti Singh, editors, *Proceedings of the 37th International Conference  
434 on Machine Learning*, volume 119 of *Proceedings of Machine Learning Research*, pages  
435 4182–4192. PMLR, 13–18 Jul 2020. [5](#)
- 436 [12] Minbeom Kim, Kyeongha Rho, Yong-duk Kim, and Kyomin Jung. Action-driven contrastive  
437 representation for reinforcement learning. *PLOS ONE*, 17(3):1–14, 03 2022. [5](#)
- 438 [13] Michael Laskin, Aravind Srinivas, and Pieter Abbeel. CURL: Contrastive unsupervised repre-  
439 sentations for reinforcement learning. In Hal Daumé III and Aarti Singh, editors, *Proceedings  
440 of the 37th International Conference on Machine Learning*, volume 119 of *Proceedings of  
441 Machine Learning Research*, pages 5639–5650. PMLR, 13–18 Jul 2020. [5](#), [7](#)
- 442 [14] Seunghyun Lee, Younggyo Seo, Kimin Lee, Pieter Abbeel, and Jinwoo Shin. Offline-to-  
443 online reinforcement learning via balanced replay and pessimistic q-ensemble. In *5th Annual  
444 Conference on Robot Learning*, 2021. [1](#)
- 445 [15] Yecheng Jason Ma, Shagun Sodhani, Dinesh Jayaraman, Osbert Bastani, Vikash Kumar, and  
446 Amy Zhang. VIP: Towards universal visual reward and representation via value-implicit pre-  
447 training. In *The Eleventh International Conference on Learning Representations*, 2023. [2](#),  
448 [5](#)
- 449 [16] Arjun Majumdar, Karmesh Yadav, Sergio Arnaud, Yecheng Jason Ma, Claire Chen, Sneha  
450 Silwal, Aryan Jain, Vincent-Pierre Berges, Pieter Abbeel, Jitendra Malik, Dhruv Batra, Yixin  
451 Lin, Oleksandr Maksymets, Aravind Rajeswaran, and Franziska Meier. Where are we in the  
452 search for an artificial visual cortex for embodied intelligence?, 2023. [2](#), [3](#), [5](#), [6](#), [7](#), [8](#)
- 453 [17] Bogdan Mazouze, Remi Tachet des Combes, Thang Long Doan, Philip Bachman, and R Devon  
454 Hjelm. Deep reinforcement and infomax learning. In H. Larochelle, M. Ranzato, R. Hadsell, M.F.  
455 Balcan, and H. Lin, editors, *Advances in Neural Information Processing Systems*, volume 33,  
456 pages 3686–3698. Curran Associates, Inc., 2020. [5](#)
- 457 [18] Russell Mendonca, Oleh Rybkin, Kostas Daniilidis, Danijar Hafner, and Deepak Pathak. Dis-  
458 covering and achieving goals via world models. *Advances in Neural Information Processing  
459 Systems*, 34:24379–24391, 2021. [5](#)

- 460 [19] Dipendra Misra, Mikael Henaff, Akshay Krishnamurthy, and John Langford. Kinematic state ab-  
461 straction and provably efficient rich-observation reinforcement learning. *CoRR*, abs/1911.05815,  
462 2019. [6](#)
- 463 [20] Suraj Nair, Aravind Rajeswaran, Vikash Kumar, Chelsea Finn, and Abhinav Gupta. R3m: A  
464 universal visual representation for robot manipulation. In *6th Annual Conference on Robot*  
465 *Learning*, 2022. [2](#), [5](#), [6](#), [7](#), [8](#)
- 466 [21] Simone Parisi, Aravind Rajeswaran, Senthil Purushwalkam, and Abhinav Gupta. The unsur-  
467 prising effectiveness of pre-trained vision models for control. In Kamalika Chaudhuri, Stefanie  
468 Jegelka, Le Song, Csaba Szepesvari, Gang Niu, and Sivan Sabato, editors, *Proceedings of the*  
469 *39th International Conference on Machine Learning*, volume 162 of *Proceedings of Machine*  
470 *Learning Research*, pages 17359–17371. PMLR, 17–23 Jul 2022. [7](#)
- 471 [22] Alec Radford, Jeff Wu, Rewon Child, David Luan, Dario Amodei, and Ilya Sutskever. Language  
472 models are unsupervised multitask learners. 2019. [1](#)
- 473 [23] Max Schwarzer, Ankesh Anand, Rishab Goel, R Devon Hjelm, Aaron Courville, and Philip  
474 Bachman. Data-efficient reinforcement learning with self-predictive representations. In *Interna-*  
475 *tional Conference on Learning Representations*, 2021. [7](#)
- 476 [24] Max Schwarzer, Nitarshan Rajkumar, Michael Noukhovitch, Ankesh Anand, Laurent Charlin,  
477 R Devon Hjelm, Philip Bachman, and Aaron Courville. Pretraining representations for data-  
478 efficient reinforcement learning. In A. Beygelzimer, Y. Dauphin, P. Liang, and J. Wortman  
479 Vaughan, editors, *Advances in Neural Information Processing Systems*, 2021. [7](#)
- 480 [25] Ramanan Sekar, Oleh Rybkin, Kostas Daniilidis, Pieter Abbeel, Danijar Hafner, and Deepak  
481 Pathak. Planning to explore via self-supervised world models. In *International Conference on*  
482 *Machine Learning*, pages 8583–8592. PMLR, 2020. [5](#)
- 483 [26] Younggyo Seo, Danijar Hafner, Hao Liu, Fangchen Liu, Stephen James, Kimin Lee, and Pieter  
484 Abbeel. Masked world models for visual control. In *CoRL*, volume 205 of *Proceedings of*  
485 *Machine Learning Research*, pages 1332–1344. PMLR, 2022. [4](#)
- 486 [27] Adam Stooke, Kimin Lee, Pieter Abbeel, and Michael Laskin. Decoupling representation  
487 learning from reinforcement learning. In *International Conference on Machine Learning*, pages  
488 9870–9879. PMLR, 2021. [1](#)
- 489 [28] Adam Stooke, Kimin Lee, Pieter Abbeel, and Michael Laskin. Decoupling representation  
490 learning from reinforcement learning. In Marina Meila and Tong Zhang, editors, *Proceedings*  
491 *of the 38th International Conference on Machine Learning*, volume 139 of *Proceedings of*  
492 *Machine Learning Research*, pages 9870–9879. PMLR, 18–24 Jul 2021. [5](#), [7](#)
- 493 [29] Yanchao Sun, Shuang Ma, Ratnesh Madaan, Rogerio Bonatti, Furong Huang, and Ashish  
494 Kapoor. SMART: Self-supervised multi-task pretraining with control transformers. In *The*  
495 *Eleventh International Conference on Learning Representations*, 2023. [3](#), [5](#), [6](#), [7](#)
- 496 [30] Yanchao Sun, Ruijie Zheng, Xiyao Wang, Andrew E Cohen, and Furong Huang. Transfer RL  
497 across observation feature spaces via model-based regularization. In *International Conference*  
498 *on Learning Representations*, 2022. [5](#)
- 499 [31] Yuval Tassa, Yotam Doron, Alistair Muldal, Tom Erez, Yazhe Li, Diego de Las Casas, David  
500 Budden, Abbas Abdolmaleki, Josh Merel, Andrew Lefrancq, Timothy Lillicrap, and Martin  
501 Riedmiller. Deepmind control suite, 2018. [3](#), [6](#)
- 502 [32] Aaron van den Oord, Yazhe Li, and Oriol Vinyals. Representation learning with contrastive  
503 predictive coding, 2019. [3](#), [5](#)

- 504 [33] Yao Wei, Yanchao Sun, Ruijie Zheng, Sai Vemprala, Rogerio Bonatti, Shuhang Chen, Ratnesh  
505 Madaan, Zhongjie Ba, Ashish Kapoor, and Shuang Ma. Is imitation all you need? generalized  
506 decision-making with dual-phase training. *arXiv preprint arXiv:2307.07909*, 2023. 5
- 507 [34] Tete Xiao, Ilija Radosavovic, Trevor Darrell, and Jitendra Malik. Masked visual pre-training for  
508 motor control, 2022. 5, 7
- 509 [35] Denis Yarats, Rob Fergus, Alessandro Lazaric, and Lerrel Pinto. Reinforcement learning  
510 with prototypical representations. In *International Conference on Machine Learning*, pages  
511 11920–11931. PMLR, 2021. 5
- 512 [36] Denis Yarats, Rob Fergus, Alessandro Lazaric, and Lerrel Pinto. Mastering visual continuous  
513 control: Improved data-augmented reinforcement learning. In *International Conference on*  
514 *Learning Representations*, 2022. 6, 9, 10
- 515 [37] Tianhe Yu, Deirdre Quillen, Zhanpeng He, Ryan Julian, Karol Hausman, Chelsea Finn, and  
516 Sergey Levine. Meta-world: A benchmark and evaluation for multi-task and meta reinforcement  
517 learning. In *Conference on Robot Learning (CoRL)*, 2019. 3, 6
- 518 [38] Zhecheng Yuan, Zhengrong Xue, Bo Yuan, Xueqian Wang, YI WU, Yang Gao, and Huazhe  
519 Xu. Pre-trained image encoder for generalizable visual reinforcement learning. In S. Koyejo,  
520 S. Mohamed, A. Agarwal, D. Belgrave, K. Cho, and A. Oh, editors, *Advances in Neural*  
521 *Information Processing Systems*, volume 35, pages 13022–13037. Curran Associates, Inc., 2022.  
522 5
- 523 [39] Amy Zhang, Rowan Thomas McAllister, Roberto Calandra, Yarín Gal, and Sergey Levine.  
524 Learning invariant representations for reinforcement learning without reconstruction. In *Inter-*  
525 *national Conference on Learning Representations*, 2021. 5
- 526 [40] Ruijie Zheng, Xiyao Wang, Yanchao Sun, Shuang Ma, Jieyu Zhao, Huazhe Xu, Hal Daumé III,  
527 and Furong Huang. TACO: Temporal latent action-driven contrastive loss for visual reinforcement  
528 learning. In *Thirty-seventh Conference on Neural Information Processing Systems*, 2023. 2, 3, 5